The Role of Neutrophils in Measles Virus–mediated Oncolysis Differs Between B-cell Malignancies and Is Not Always Enhanced by GCSF

Aditi Dey[1], Yu Zhang[2], Anna Z Castleton[3], Katharine Bailey[1], Brendan Beaton[1], Bella Patel[4] and Adele K Fielding[1]

[1]Cancer Institute, University College London, London, UK; [2]Department of Laboratory Medicine, Harvard Medical School and Children's Hospital Boston, Boston, Massachusetts, USA; [3]Department of Haemato-Oncology, St. Bartholomews Hospital, West Smithfield, London, UK; [4]Barts Cancer Institute, The London School of Medicine, Queen Mary University of London, London, UK

The mechanism by which oncolytic measles virus (MV) kills cancer cells remains obscure. We previously showed that neutrophils are involved in MV-mediated tumor regressions and become activated, upon MV infection. In the present study, we attempted to enhance the neutrophil response toward MV-infected tumor targets by generating an oncolytic MV-expressing human granulocyte colony-stimulating factor (MVhGCSF). Evaluating the effects in two different models of B-cell malignancy, we showed that depletion of neutrophils abrogated the MV therapeutic effect in an *in vivo* Raji—but not Nalm-6 tumor model. Next, we compared MVhGCSF with the unmodified backbone virus MVNSe. MVhGCSF enhanced the oncolytic capacity of MV in the Raji model *in vivo*, whereas in the Nalm-6 model, the opposite was unexpectedly the case. This finding was recapitulated by exogenously administered hGCSF. MVhGCSF replicated within an MV-infectable CD46 transgenic mouse model with detectable serum levels of hGCSF but no toxicity. Our data suggest that a "one-size-fits-all" model of immune response to viral oncolysis is not appropriate, and each tumor target will need full characterization for the potential of both direct and indirect, innate immune responses to generate benefit.

Received 12 February 2015; accepted 10 August 2015; advance online publication 22 September 2015. doi:10.1038/mt.2015.149

INTRODUCTION

The Edmonston-B derived vaccine strain of measles virus (MV) is oncolytic in various tumor models *in vivo* and is currently being tested in several phase 1 trials. MV is naturally lymphotropic, and B-cell malignancies appear particularly sensitive.[1,2] In an ongoing clinical trial in patients with relapsed, multiple myeloma, two complete remissions were observed.[3]

In addition to the direct oncolytic effect of MV, our work has shown that neutrophils are involved in MV-mediated tumor regressions.[4] Furthermore, neutrophils from healthy donors became activated upon oncolytic (but not wild-type) MV infection and survived significantly longer in culture. Upon oncolytic MV infection, neutrophils produced various antitumor cytokines as well as degranulation markers in response to infection, resulting in the release of tumor necrosis factor (TNF)-related apoptosis inducing ligand (TRAIL) directly from preformed granules.[5]

Neutrophils have also been implicated in various other microorganism-mediated tumor regressions.[6,7] In a bladder cancer model, where BCG (Mycobacterium bovis bacillus Calmette–Guerin) was used as a treatment, neutrophils were shown to play a key role in therapy.[8] In a model of murine colon adenocarcinoma which was treated with vesicular stomatitis virus, shutdown of blood flow to the tumors was observed, which was proposed to be mediated by neutrophils.[9] The shutdown of the blood flow to the tumors led to apoptosis in even those tumor cells that were not infected by the vesicular stomatitis virus. It was also shown that vesicular stomatitis virus attacks the tumor vasculature and induces clot formation that correlates with decrease in tumor cell proliferation.[10] In a metastatic breast cancer model, MV expressing the neutrophil-activated protein of Helicobacter pylori led to improved antitumor activity with an increased Th1 type cytokine response.[11]

In the present study, we aimed to enhance the therapeutic efficacy of MV by expressing the human granulocyte colony-stimulating factor (hGCSF), known to stimulate the survival, proliferation, and cytotoxic function of neutrophils both *in vitro* and *in vivo*,[12] as an additional transcription unit of MV. Murine and human GCSF share 73% amino acid sequence homology and full cross-reactivity[13] and hence can be tested in both human and murine experimental systems. We predicted that expression of GCSF by MV-infected target cells would enhance the antitumor properties of neutrophils *in vivo* and lead to augmentation in tumor regressions. We chose two tumor models of aggressive B-cell malignancy because of their different responses to MV oncolysis in our hands. Raji—Burkitt lymphoma-derived tumors—respond to MV therapy but less quickly and completely than does the Nalm-6 model, which is derived from acute lymphoblastic leukemia.[1,2]

Our data suggest that neutrophils can play very different roles in MV-mediated effect *in vivo* in different tumor models.

Correspondence: Adele K Fielding, Cancer Institute, University College London, 72 Huntley St, London WCIE 6DD, London, UK.
E-mail: a.fielding@ucl.ac.uk

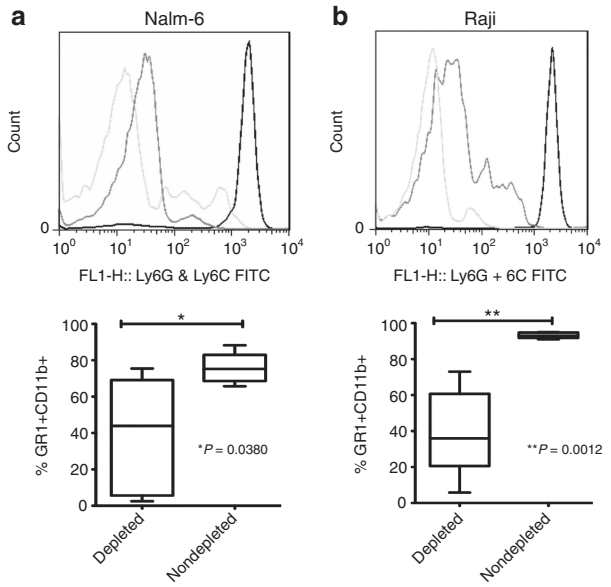

Figure 1 Confirmation of neutrophil depletion by flow cytometry. Peripheral blood was analyzed by flow cytometry for neutrophil depletion using anti-GR1 and anti-CD11b antibodies in mice bearing (**a**) Nalm-6 and (**b**) Raji tumor. For each tumor type, representative histograms plots are shown in the upper panels (light gray line = isotype control, dark gray line = depleted group, black line = nondepleted group) and in the lower panel box plots showing aggregate data of percentage CD11b GR1 positive cells in (**a**) Nalm-6 and (**b**) Raji models. (**a**) Nalm-6 tumors (43.92 median in depleted and 75.25 median in nondepleted) and (**b**) Raji tumors (35.93 median in depleted and 93.05 median in nondepleted) in the depleted (Nalm-6 ($N = 5$); $N = 5$ Raji ($N = 5$)) and nondepleted. FITC, fluorescein isothiocyanate.

RESULTS

Neutrophil depletion *in vivo* abrogates MV therapeutic effect in Raji but not Nalm-6

We hypothesized that, if neutrophils are playing a role in MV oncolysis *in vivo*, then depletion should abrogate the MV-mediated oncolytic effect *in vivo*. We treated Raji and Nalm-6 SCID subcutaneous xenografts of B-cell malignancy, both of which are known to respond to MV therapy to different degrees with MV by i.t. injection from day 1 after significant neutrophil depletion was confirmed by fluorescence activated cell sorting (FACS; **Figure 1**). The Nalm-6 tumors regressed rapidly and completely after MV injection in both depleted ($N = 9$) and nondepleted group ($N = 8$), and there was no difference in tumor size between the cohorts (**Figure 2a**). By contrast, the Raji tumors responded less well in the neutrophil depleted group ($N = 8$) than the nondepleted group ($N = 9$)—all mice in the depleted group had reached the humane end point (tumor size 2.5 mm^3 and/or hind limb paralysis) at 27 days, whereas only half in the nondepleted group (**Figure 2b**). There was a significant difference ($P = 0.0001$) in the survival between the two groups in the Raji (**Figure 2c**) but not in the Nalm-6 model (**Figure 2d**). The data suggested that the neutrophil-mediated enhancement of MVs oncolytic activity is likely to play a more prominent role where the direct antitumor effect is less pronounced as observed in the Raji model.

Human GCSF can be expressed as an additional transcription unit of MV

To enhance the antitumor function of neutrophils, we cloned the gene encoding hGCSF, as an additional transcription unit of MVNSe (**Figure 3a**). MVhGCSF was rescued successfully from cloned DNA and a one-step growth curve (**Figure 3b**) performed on Vero cells showed a similar growth pattern and viral titers to the parent MVNSe (10^6 and 10^7 plaque-forming unit (PFU)). Human GCSF protein, quantified by enzyme-linked immunosorbent assay (ELISA) after infection of Raji and Nalm-6 cells (**Figure 3c**) as well as neutrophils freshly isolated from healthy donors (**Figure 3d**) accumulated to a level of 100–300 ng/ml after infection of the cell lines over 5 days and 2–3 ng/ml after infection of the neutrophils for 24 hours. No hGCSF was produced by control infected or uninfected cells.

MVhGCSF is therapeutic in Raji and Nalm-6 subcutaneous xenografts

To determine the therapeutic effect of expressing hGCSF by MV *in vivo*, we compared the therapeutic efficacy of MVNSe with that of MVhGCSF in subcutaneous models of both Nalm-6 and Raji tumors. After tumors reached 0.2–0.4 cm^3 (**Figure 4a**,**b**), we gave 10 i.t. injections of MVNSe ($N = 5$), MVhGCSF ($N = 6$), or UV-irradiated nonreplicating MV control (MVUV) ($N = 7$). In the Raji model, MVhGCSF treatment generated a highly significantly superior ($P = 0.0001$) antitumor effect by comparison to MVNSe (**Figure 4c**), and Kaplan–Meier analysis showed that the MVhGCSF-treated mice survived significantly longer than MVNSe-treated mice ($P = 0.0098$; **Figure 4e**). In the Nalm-6 model, both MVhGCSF and MVNSe resulted in complete regression of the tumors in both cohorts (**Figure 4d**), and all mice survived, tumor free in both groups, hence there was no survival advantage to MVhGCSF (**Figure 4f**).

MVhGCSF play different roles in Raji and Nalm-6 disseminated xenografts

B-cell malignancies are disseminated diseases—we used i.v.-injected Nalm-6 and Raji tumor cells expressing luciferase (luc), to enable *in vivo* monitoring of disease progression. Mice received 6 weekly injections of 10^6 PFU of MVNSe ($N = 7$), MVhGCSF ($N = 6$), or MVUV ($N = 3$) and an additional control of hGCSF alone, using pegylated hGCSF (Peg hGCSF) ($N = 5$) at 120 µg/kg. In the Raji luc model, only three of the six planned weekly injections of 10^6 PFU of MVNSe ($N = 10$), MVhGCSF ($N = 10$), MVUV ($N = 8$), and Peg hGCSF ($N = 9$) were possible before the mice succumbed.

Figure 5 shows weekly *in vivo* images in the Nalm-6 luc (**Figure 5a**) and Raji luc (**Figure 5b**) experiments. In the Nalm-6 luc model (**Figure 5a**), the two nontherapeutic/control groups MVUV and Peg hGCSF (**Figure 5(a(i))**) and the two therapeutic/experimental groups MVNSe and MVhGCSF (**Figure 5(a(ii))**) were carried out at slightly different times, so the luciferase signal can only be appropriately compared between those groups imaged at the same time, due to threshold setting. In the Nalm6 luc model, we detected signal as early as week 2 in Peg hGCSF-treated group when compared to the MVUV-treated group, and by week 6 in the Peg hGCSF treated group, two of five mice had to be taken down (**Figure 5(a(i))**). Similarly, in the Nalm-6 luc model, MV therapeutic groups, we detected signal at week 5 in the MVhGCSF-treated group when compared to the MVNSe-treated group and by week 10, two of six mice had to be taken down (**Figure 5(a(ii))**).

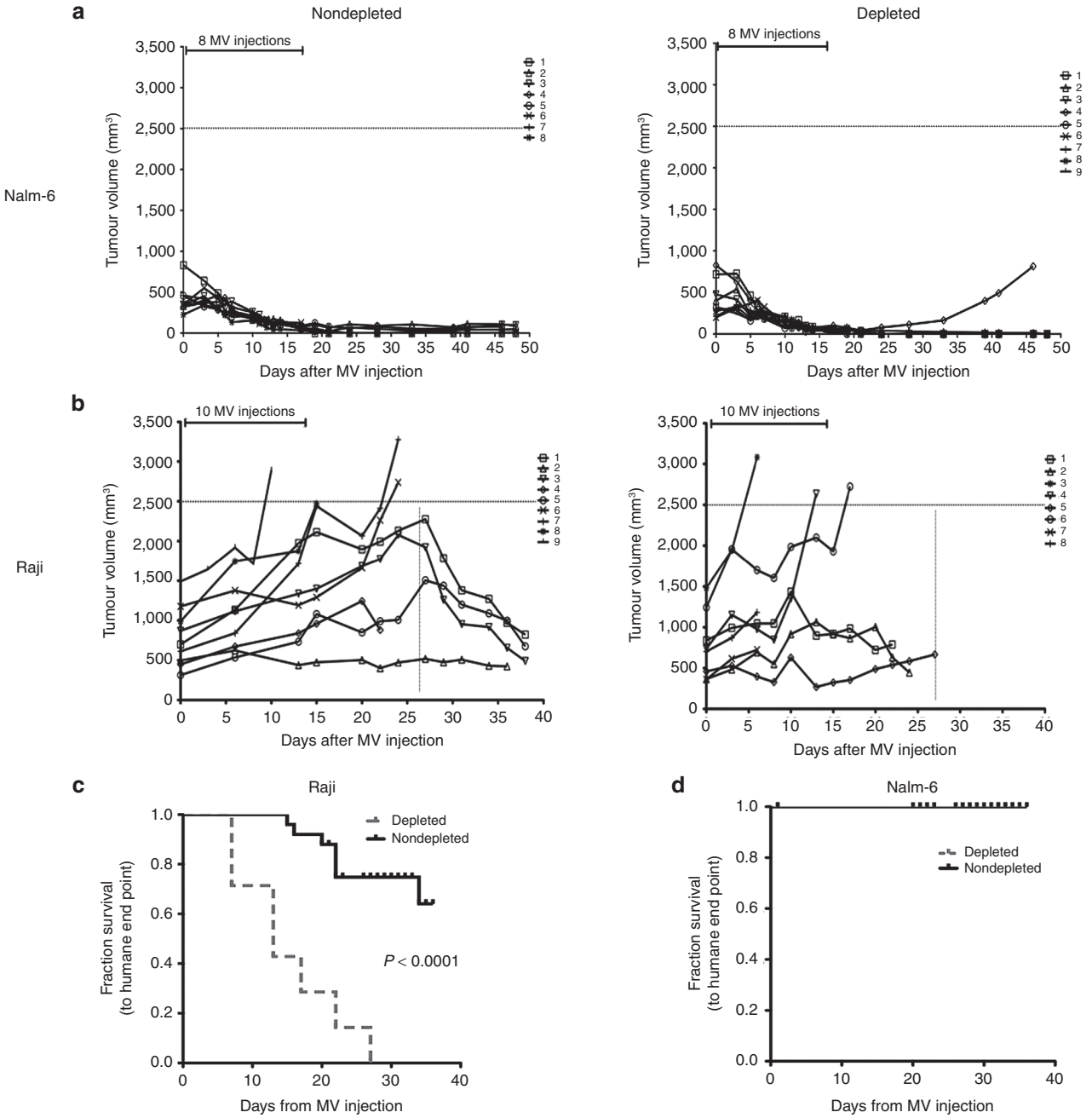

Figure 2 Neutrophil depletion abrogates MV-mediated oncolysis in Raji but not Nalm-6 model *in vivo*. (**a**) Graphs showing tumor volumes in individual mice in Nalm-6 (nondepleted (*N* = 8); depleted (*N* = 9)) and (**b**) Raji (nondepleted (*N* = 9); depleted (*N* = 8)) after MV treatment. Kaplan–Meier survival curves in the (**c**) Raji model and (**d**) Nalm-6 model are shown with solid line representing the nondepleted group and dashed line representing the depleted group. Statistical analysis was performed using log-rank test to obtain the *P* value.

We quantified total signal by plotting individual values for luminescence (photons/second) performed on each surviving animal in the nontherapeutic groups at week 6 (**Figure 5c**) and the therapeutic groups at week 10 (**Figure 5d**). The data showed significant difference between the groups with a higher tumor burden in the mice who had received any therapy including GCSF (either the peg hGCSF control or MVhGCSF). In the Raji luc model (**Figure 5b**), signal was detected at week 2. Quantification of total signal (**Figure 5e**) at week 2 showed that, by contrast to the Nalm-6 luc model, the MVhGCSF treated mice had significantly lower tumor burden compared to the MVNSe-treated group.

Figure 6 compares the survival of the mice in the two different models—Nalm-6 luc (**Figure 6a–d**) and Raji luc (**Figure 6e–h**). The Kaplan–Meier curves (**Figure 6a**) illustrate that, in the Nalm-6 luc model, mice treated with the controls alone succumbed to leukemia the most quickly; the survival was least good in the group treated with GCSF alone, where the median survival was 50 days compared to 75 days in the MVUV-treated group ($P = 0.0120$). Seventy-five percent of the mice treated with MVNSe responded and were alive at the end of the experiment. Surprisingly, mice receiving treatment with MVhGCSF had a significantly inferior outcome with median survival of 78.5 days compared to the MVNSe-treated

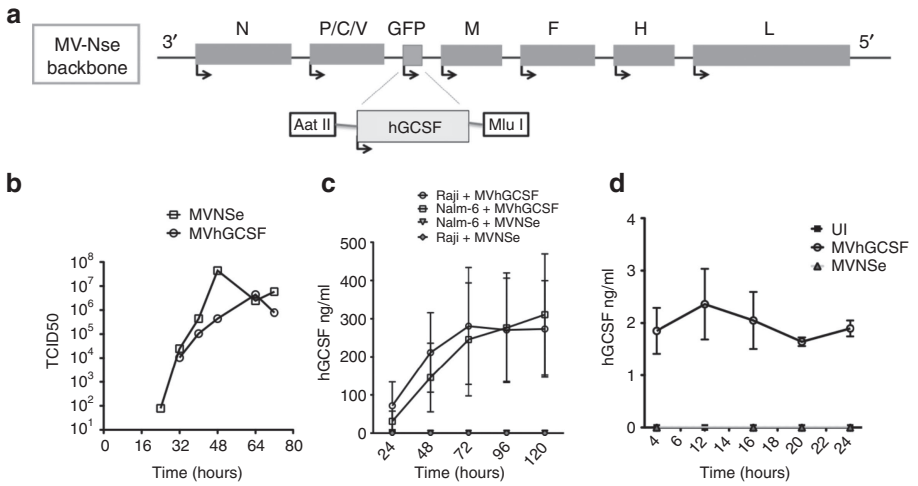

Figure 3 Construction and characterization of MV-expressing hGCSF. (**a**) Schematic showing cloning of DNA encoding human cytokine granulocyte colony-stimulating factor (hGCSF) p (+) MV-NSe upstream of M, using AatII and MluI restriction enzymes. (**b**) One step growth curve of MVhGCSF performed on Vero cells (circles, MVhGCSF; squares, MVNSe). (**c**) hGCSF quantitation in supernatant of Nalm-6 infected with MVhGCSF (squares) or MVNSe (inverted triangles) ($N = 3$) and supernatant of Raji infected with MVhGCSF (circles) or MVNSe (diamonds) ($N = 3$). (**d**) hGCSF quantitation in supernatant of neutrophils from healthy donors infected with MVhGCSF (circles), MVNSe (triangles), or mock infected (filled squares) ($N = 3$).

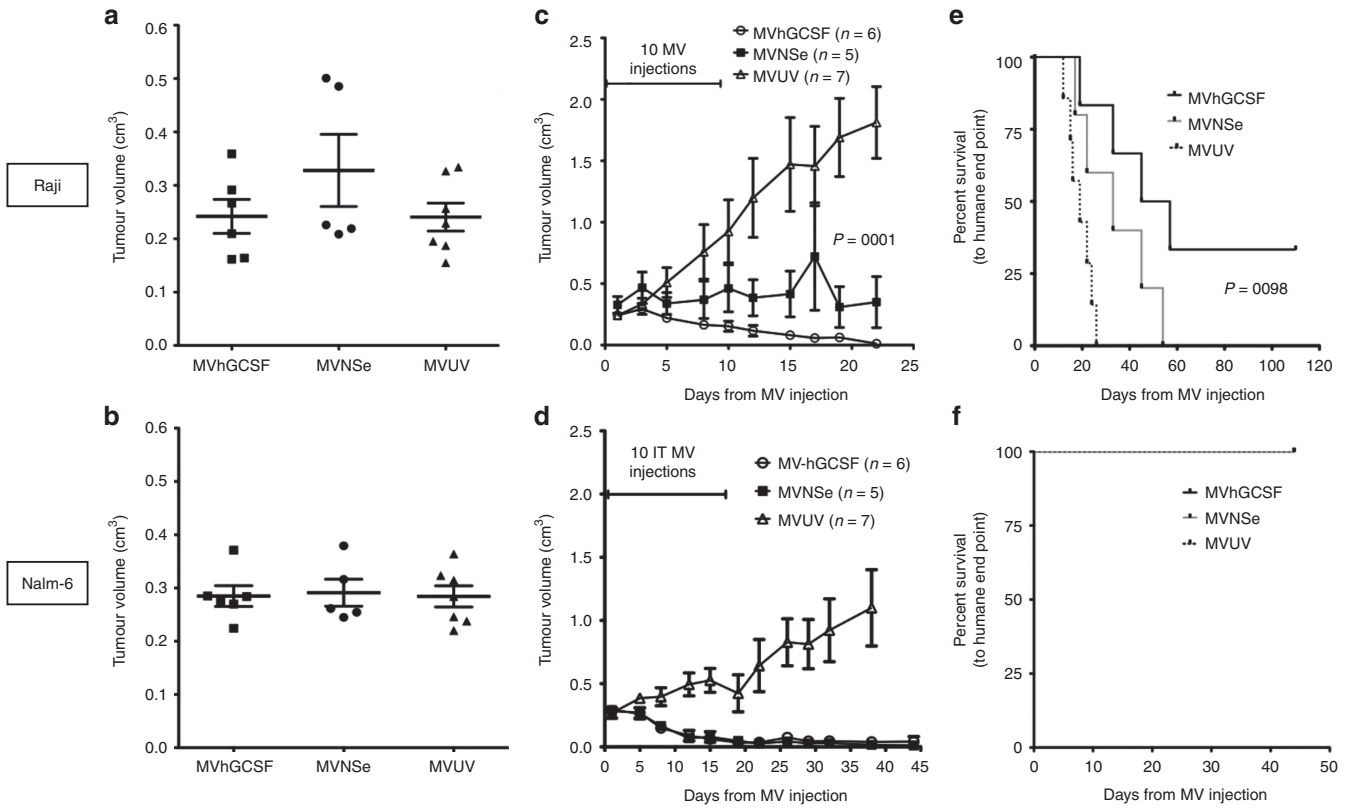

Figure 4 MVhGCSF is therapeutic in two different subcutaneous B-cell malignancies. (**a, c, e**) Raji and (**b, d, f**) Nalm-6 xenografts were established subcutaneously in SCID mice. Tumor volumes before commencing the MV injections are shown in **a** and **b**. Tumor volume measurement was documented after MV-hGCSF (circles), MV-NSe (filled squares), and MVUV (triangles) injections in both the models **c** and **d**. **e** and **f** shows the Kaplan–Meier survival plots in MVhGCSF (black lines), MVNSe (gray lines) and MVUV (dotted lines) treated cohorts. MVhGCSF, $N = 6$; MVNSe, $N = 5$; MVUV, $N = 7$. Mann–Whitney and log rank statistical tests were performed to get the P values. SCID, severe combined immunodeficiency.

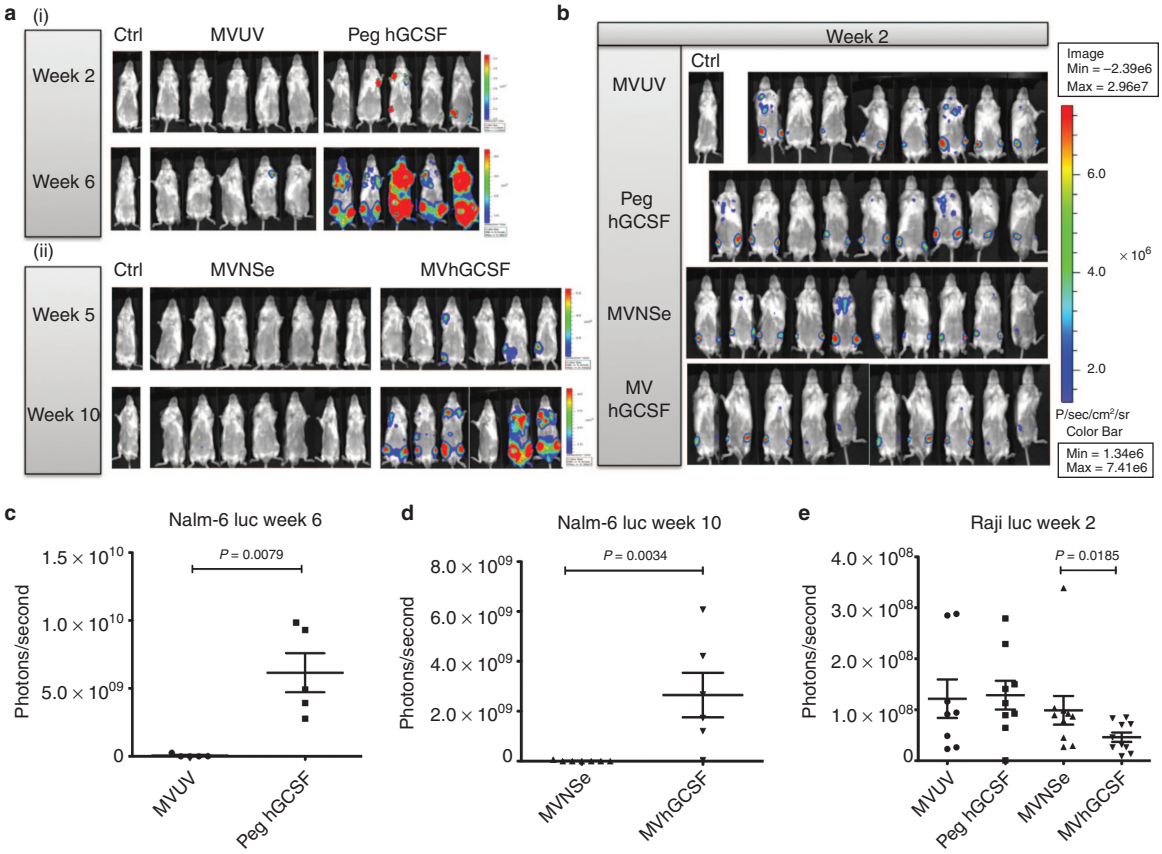

Figure 5 *In vivo* imaging of Nalm-6 and Raji luciferase disseminated SCID model. Bioluminescent images showing comparison of leukemia signal in Nalm-6 model; (**a**(i)) nontherapeutic MVUV (middle panel) and Peg hGCSF (right panel) groups at week 2 and week 6 post tumor inoculation and (**a**(ii)) therapeutic MVNSe (middle panel) and MVhGCSF (right panel) groups at week 5 and week 10 post tumor inoculation. Both a(i) and a(ii) images were taken with PBS-injected controls (Ctrl) to account for background luminescence. The scales are next to the set of images compared at each week. (**b**) Bioluminescent images comparing all the groups in the Raji luciferase model at week 2, post tumor inoculation, images were taken with PBS-injected control (Ctrl) to account for background luminescence. The scale is on the right side of the image. Quantification of tumor burden using bioluminescence. (**c, d, e**). Scatter dot plot showing individual values for luminescence (photons/second) performed on each surviving animal in each treatment group at week 6 (Nalm-6 luc nontherapeutic groups) (**c**), week 10 (Nalm-6 luc therapeutic group) (**d**), and week 2 (Raji luc) (**e**). Values are represented minus background activity. Data shown are mean ± SEM. PBS, phosphate buffered saline; SCID, severe combined immunodeficiency.

cohort—median not reached by the end of the experiment (P = 0.0149; Figure 6a). At humane end point, presence of CD10CD19 cells in the bone marrow (BM) confirmed presence of leukemia (Figure 6b). hGCSF was detected at comparable levels in the serum of the peg hGCSF- and MVhGCSF-treated cohorts confirming the appropriate dosing of the exogenously administrated peg hGCSF (Figure 6c). There was no significant difference in total cell numbers recovered from the spleens (MVNSe: mean = 2.338, range: 2.0–2.675 million; MVhGCSF: mean = 5.922, range: 0.625–25.0 million; MVUV: mean = 2.275; range: 0.5–2.275 million; Peg hGCSF: mean = 4.450, range: 1.75–8.5 million), indicating that hyperleucocytosis was not the cause of increased death in the MVhGCSF-treated acute lymphoblastic leukemia (ALL) mice. FACS analysis of %GR1+ neutrophils (Figure 6d) and % NK and Mac3 (**Supplementary Figure S1a**) did not show any difference between the groups. These data indicate that expression of hGCSF by MV results in a much poorer survival of Nalm-6 ALL leukemic mice compared to MVNSe and that this is due to enhanced tumor progression.

In the Raji luc model (Figure 6e–h), the disease progressed very quickly in all the groups. The Kaplan–Meier survival curve (Figure 6e) shows that by day 32, all the mice had reached their humane end point. CD19CD20 positivity confirmed death due to leukemia (Figure 6f). We detected very high levels of hGCSF in the serum of the mice treated with MVhGCSF and Peg hGCSF (Figure 6g). This correlated with significantly higher levels of GR1+ neutrophils in the spleen of these mice (Figure 6h). Significantly higher levels of macrophage infiltration in the spleens of MVhGCSF treated mice was also observed when compared to the MVNSe treated groups (**Supplementary Figure S1b**).

MVhGCSF does not enhance proliferation *in vitro*

To ensure that the *in vivo* data we collected did not simply result from a direct effect of GCSF on cell proliferation, we treated the cell lines with increasing concentrations of recombinant hGCSF *in vitro* and enumerated the cells over 4 days (Figure 7a). We did not observe any difference between GCSF-treated and control cell lines *in vitro*.

MVhGCSF in MV-infectable, CD46 transgenic mice is not toxic

Finally, we evaluated MVhGCSF in CD46 transgenic mice in which all cells, not just tumor cells, are infectable by MV. To assess this,

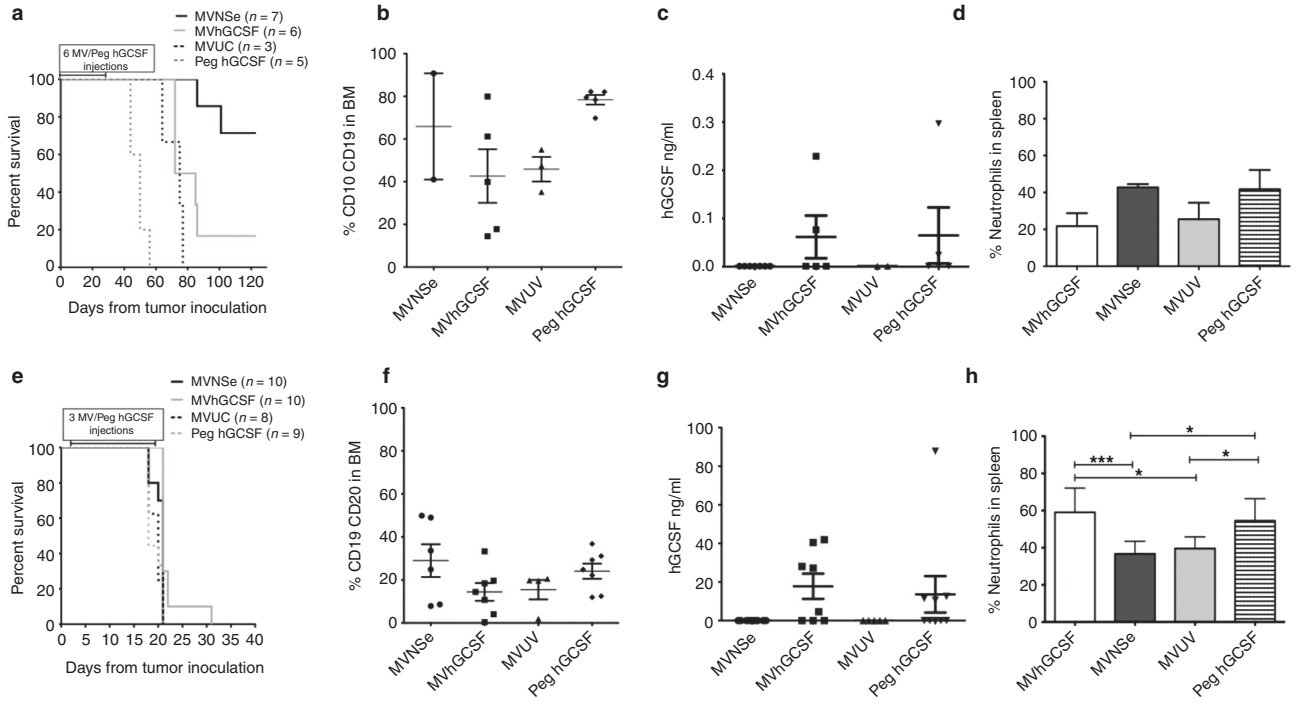

Figure 6 Effects of MVhGCSF is different in two different disseminated models of B cell malignancy. (**a** and **e**) Kaplan–Meier survival curve showing MVhGCSF (gray line), MVNSe (black line), MVUV (black dotted line) and Peg hGCSF (gray dotted line) treated mice. At humane end point (hind limb paralysis), the presence of disease was confirmed by flow cytometry by %CD10CD19 (**b**) and %CD19CD20 (**f**) in the BM compartment of Nalm-6 and Raji models, respectively. The level of hGCSF in the serum of the mice (**c** and **g**) was quantified by ELISA. (**d** and **h**) Percentage of neutrophils in the spleens was determined by flow cytometry—MVhGCSF (median 59.88), MVNSe (median 37.41), MVUV (median 39.64), and Peg hGCSF (median 59.48) (MVhGCSF versus MVNSe; $P = 0.0006$) (MVhGCSF vs. MVUV; $P = 0.0121$) (MVNSe versus Peg hGCSF; $P = 0.0262$). ***$P < 0.001$; *$P \leq 0.04$. All data shown are mean ± SEM. BM, bone marrow; ELISA, enzyme-linked immunosorbent assay.

Ifnar^{KO} × CD46Ge mice[14] were injected i.v. with either MVNSe or MVhGCSF. They were monitored for 35 days after which spleen size, differential cell count in spleen (NK, macrophage, neutrophil percentages), and serum hGCSF levels were determined. There was no difference in spleen size (**Figure 7b**) or cellular contents in the spleen between the groups (**Figure 7c**). None of the mice became unwell. The mice treated with MVhGCSF showed hGCSF in the serum at day 35 (**Figure 7d**), but there was no toxicity. These data suggest that any adverse effect of expressing hGCSF as an additional transcription unit in Nalm-6 disseminated mice relates solely to promotion of tumor growth and not to toxicity of GCSF production.

DISCUSSION

Innate immunity, which will be less compromised by and quicker to recover after anticancer chemotherapy, may play a pivotal role in viral oncolysis. Taking into account our previous work, in which we have clearly demonstrated that oncolytic MV enhance neutrophil antitumor properties, we attempted to augment these properties by generating MVhGCSF.

In our initial neutrophil depletion experiments, the therapeutic effect of MV in the Raji model was significantly abrogated, whereas in the Nalm-6 ALL subcutaneous model, depletion of neutrophils did not abrogate the 100% response rate. A possible explanation is that the Nalm-6 tumors simply regressed so rapidly compared to the Raji tumors, that the direct oncolytic effect of MV in the Nalm-6 tumors superseded any involvement of neutrophils *in vivo*. However, it is also possible that the individual targets are differentially responsive to neutrophil effects.

In the *in vivo* subcutaneous tumor models, we found that MV-expressing hGCSF had a significantly superior therapeutic effect to MVNSe in the Raji model but was equivalently good at tumor eradication to MVNSe in the Nalm-6 model, both in the proportion of responding tumors and time to response, consistent with our expectations from the neutrophil depletion experiments.

As B-cell malignancies are disseminated diseases, we established systemic tumor models of Nalm-6 and Raji and then tested the therapeutic efficacy of the MV-expressing human GCSF in a systemic therapeutic approach by delivering the treatment intravenously. In disseminated Nalm-6 xenografts, our previous data showed that ~60% of mice have complete regression of the tumors with i.v. delivered MV[2] offering a greater probability to observe any potential therapeutic benefit to MVhGCSF. In the Raji model, our previous data showed that neutrophils could play a beneficial role in improving therapeutic efficacy of MV[4]. Surprisingly, in the Nalm-6 disseminated model, not only was there no benefit to MVhGCSF, but there was an increased rate of death in those mice, which also occurred with the pegylated hGCSF alone control conditions. We confirmed that the levels of GCSF detected in the mouse sera were almost identical between exogenously administered and GCSF produced by administration of MVhGCSF suggesting an active, productive infection of tumor targets. We confirmed that disease progression rather than GCSF toxicity was responsible for these observations and further analysis showed that the immune cell

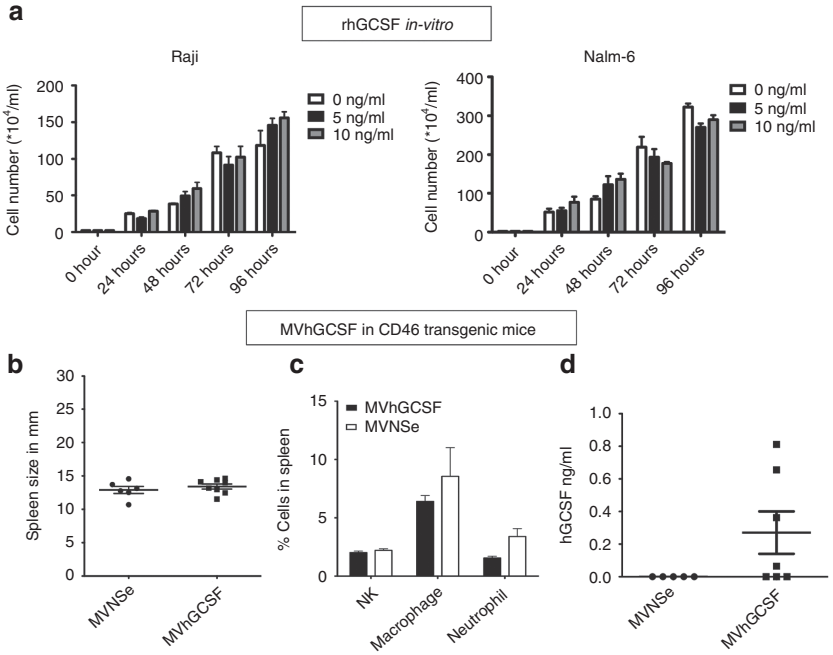

Figure 7 Recombinant hGCSF does not proliferate tumor cells *in vitro* and MVhGCSF is not toxic in Ifnar^{ko} × CD46 Ge mice permissible to MV infection. (**a**) Raji and (**b**) Nalm-6 cells were treated with increasing amounts of rhGCSF and counted every 24 hours by trypan blue exclusion method *in vitro*. The number of cells/ml is plotted against the time. CD46 transgenic mice were injected intravenously with MV-NSe (N = 5) or MVhGCSF (N = 7). Evaluation was carried out at day 35 after injection. (**b**) Spleen size in mm. (**c**) The percentage of NK cells macrophages and neutrophils in the spleens. (**d**) Serum hGCSF levels in ng/ml.

composition of the spleens from MVNSe and MVhGCSF did not differ, especially, there was no excess of neutrophils, ruling out direct toxicity of GCSF. Lack of toxicity in the CD46 transgenic model confirms this. In the Raji disseminated model, the disease progressed very rapidly in all the groups. By third week, all of them had succumbed to hind limb paralysis and had to be sacrificed. In contrast to the Nalm-6 model, the Raji disseminated model showed significantly high level of infiltrating neutrophils in the spleen of the mice treated with MVhGCSF or Peg hGCSF when compared to the MVNSe and MVUV treated groups. Human GCSF levels in the serum of these mice were also very high. At week 2, we observed some therapeutic benefit of using MVhGCSF over MVNSe by the live *in vivo* imaging quantification (**Figure 5e**), but this was short lived. The percentage of tumor cells in the BM of the mice at the time of death was similar all across the groups (**Figure 6f**), whereas in the Nalm-6 model, the peg hGCSF-treated group had significantly high level of tumor cells in their BM in comparison to the other groups at the time of death (**Figure 6b**), which again shows a proliferating effect of GCSF on Nalm-6 cells *in-vivo*. But this effect was not there on the Raji cells *in vivo*.

We believe that the Raji model can benefit from use of MVhGCSF, as neutrophils have consistently shown to play a role in MV-mediated oncolysis in this model. We think that we observed a short-term benefit in this model because we kept the tumor cell inoculation dose (1 million cells) and the schedule of weekly injections of MV therapy similar to that of the Nalm-6 model, to be able to directly compare the two models. As Raji is more aggressive than the Nalm-6 model, with lowering of tumor inoculation dose and increasing the therapeutic dose and frequency of MV, we might be able to see a more robust therapeutic benefit.

GCSF is widely used in the clinical treatment of patients with aggressive B-cell malignancies and has been shown to improve outcome,[15] although it is long known that GCSF can also facilitate mobilization of tumor from the bone marrow niche.[16] However, preclinical studies of the CXCR4 antagonist plerixafor, typically used in conjunction with GCSF, have shown promising results in *in vivo* models of primary ALL, suggesting that bone marrow microenvironment disruption may be therapeutically beneficial[17,18] by increasing chemosensitivity of resistant, possibly quiescent, leukemia, clones after removal from their niche. A clinical trial NCT01331590 is being conducted, evaluating the role of GCSF in priming the bone marrow of ALL patients for subsequent chemotherapy targeting.[19] By contrast, GCSF accelerated disease progression in a subset of primary ALL patient xenografts in NSG mice.[20] No evidence for a direct mitogenic effect of GCSF could be demonstrated in any of the xenografts using exogenous GCSF *in vitro*. Also, quiescent leukemia cells can be induced to enter the cell cycle by treatment with GCSF[21] and then targeted by chemotherapy.

We showed that MVhGCSF has superior potency to MVNSe as an oncolytic agent in the Raji model, also generating clinically therapeutic serum GCSF levels.[22] However, Nalm-6 ALL showed unexpectedly aggressive progression after MVhGCSF. Future studies would require caution as any benefit from hGCSF as expressed by oncolytic viruses could be difficult to predict and could vary from patient to patient.

MATERIALS AND METHODS

Cell lines. Vero and Raji (ATCC, UK) and Nalm-6 (DSMZ, Germany) cell lines were used. Vero was grown and maintained in Dulbecco's modified Eagle's Medium (Life Technologies, UK) (supplemented with 5% fetal bovine

serum); Raji and Nalm-6 and Nalm-6 expressing luciferase (Nalm-6 luc)[23] and Raji expressing luciferase were grown in RPMI1640 (Life Technologies, UK) (supplemented with 10% fetal bovine serum) (R10 media).

Cloning and rescue. hGCSF-expressing vector was bought from Invivogen, France. Site-directed mutagenesis was used to remove an Aat II site from the middle of the gene using Stratagene Quickchange II kit (Agilent Technologies, UK). It was then PCR amplified with the following primers, forward primer MluI+hGCSF: 5′- agtatta*acgcgt*atggctggacctgccacccagagc-3′ and reverse primer: AatII_hGCSF: 5′-tacagtc*ggacgtc*attcagggctgggcaaggtggcg-3′, and the PCR product was cloned into the MVNSe backbone using AatII and MluI restriction endonucleases (New England Biolab, UK), replacing GFP, upstream of MV M gene. The virus was rescued on Vero cells by using a MVA-T7–based system described previously.[24]

Virus propagation and titration. Both unmodified MVNSe, which is derived from the Edm B vaccine strain, and hGCSF-expressing modified MVhGCSF were propagated and titrated by $TCID_{50}$ titration on Vero cells, and one-step growth curve was performed on Vero cells and titrated as described earlier.[25]

Neutrophil isolation. Neutrophils were isolated from heparinized peripheral blood of healthy volunteers after they gave informed consent, by sedimentation with 3% dextran gradient (Fisher Scientific, Leicestershire, UK) as previously described.[5]

ELISA. hGCSF was quantified using human GCSF ELISA kit (Peprotech, UK) according to manufacturer instructions.

In vitro *recombinant human GCSF (rhGCSF) assay.* Raji and Nalm-6 cells were plated at 2×10^4/ml in T25 tissue culture flasks in R10 media supplemented with 0, 5, and 10 ng/ml rhGCSF (Peprotech, UK). The cells were incubated at 37 °C. They were counted using Trypan blue dye (Sigma Aldrich, Poole, UK) exclusion method to determine number of viable cells/ml every 24 hours.

In vivo *experiments.* All animal experiments were performed according to UK Home Office approved protocols and institutional guidelines.

***Neutrophil depletion* in vivo.** Neutrophils were depleted *in vivo* using a rat antimouse Gr-1 monoclonal antibody (anti-Ly 6G & 6C, clone RB6-8C5; R&D Biosystems, Abingdon, UK) via i.v., i.p., and/ or i.t. routes on day 0. The control mice received equivalent amount of a rat immunoglobulin ($IgG2_b$, BD Biosciences, Oxford, UK). 35–50 µg of antibody was used for i.v. or i.t. routes whereas 150µg of antibody was used for i.p. routes per dose.

Neutrophil depletion was confirmed by FACS regularly. Approximately 50 µl of peripheral blood was collected by tail vein bleed and red blood cells were removed by hypotonic lysis. The white blood cells were then stained with rat antimouse CD11b-APC (clone M1/70; BD Biosciences) and rat antimouse Ly-6G and Ly6C-FITC (clone RB6-8C5; BD Biosciences). FACS analysis was performed on the stained cells. The neutrophil depletion was repeated every 3–5 days and maintained throughout the MV therapeutic window.

Mice were injected with MV from day 1 after neutrophil depletion at multiplicity of infection of 1.0 daily i.t. in a total volume of 100 µl. A total of 8 and 10 MV injections were administered i.t. to Nalm-6 and Raji tumors, respectively. Tumor volume was calculated using the formula:

$$V = a^2b / 2mm^3$$

where a = the shortest diameter and b = the longest diameter.

Mice were euthanized by schedule 1 procedure when they reached their predetermined humane end points (tumor volume ≥2.5 cm^3 or systemic spread of disease = onset of hind limb paralysis).

Raji and Nalm-6 SCID xenografts for therapeutic experiment. Raji (Burkitt's lymphoma) and Nalm-6 (ALL) subcutaneous xenografts were established in 6–8-weeks-old CB17-$Prkdc^{scid}$ (severe combined immunodeficiency (SCID)) mice (Charles River, Margate, UK). To establish ALL xenografts, 5×10^6 viable Nalm-6 cells (ATCC, LGC, UK) were mixed with 2 µg prethawed Matrigel (BD Biosciences) in a total volume of 200 µl and injected into the right flank of each mouse. For the Raji xenografts, 10×10^6 viable Raji cells (ATCC, LGC, UK) was injected in 200 µl of RPMI 1640 medium. When the tumors reached 0.2–0.4 cm^3, they were administered with MV (MVNSe, MVUV, MVhGCSF) i.t. for a total of 10 doses at an multiplicity of infection of 1.0.

Disseminated xenografts were established by tail vein injection of 1×10^6 Nalm-6/Raji luciferase cells. Three days after tumor cell transfer 1×10^6 PFU of MV (MVNSe, MVUV, MVhGCSF) or 120 µg/kg of Pegylated hGCSF (Peg hGCSF) (Neulasta; Amgen) was administered at weekly intervals for a total of six doses for Nalm-6 and three doses for Raji. The dosage of Peg hGCSF was based on the literature.[26–29] MV was administered via the i.v. route by tail vein injection while Peg hGCSF was administered i.p.. Mice were monitored daily and euthanized when predefined humane end points were reached. At the humane end point, spleens from the mice were analyzed for the number of total cells recovered and percentage of neutrophil, macrophage, and NK cells by FACS. Serum from all these mice was collected by exsanguination and hGCSF levels were determined by ELISA.

In vivo *imaging.* Nalm-6/Raji luciferase-injected mice were imaged once a week by bioluminescent imaging. Mice were shaved and injected i.p. with 200 µl of D-luciferin (Caliper Life Sciences, Cheshire, UK). They were then imaged under anesthetic (Isofluorane) under IVIS 100 Lumina (Caliper Life Sciences, Cheshire, UK). The results were analyzed using Living Image 3.2 software.

Toxicity studies in $Ifnar^{ko}$× CD46 Ge mice. $Ifnar^{KO}$ × CD46 Ge mice were kindly provided by Roberto Cattaneo (Mayo Clinic). They were injected with 1×10^6 PFU of MVNSe or MVhGCSF i.v. via tail vein. The mice were then monitored twice a week for 35 days for any sign of ill health. On day 35, all the mice from both the cohorts were sacrificed and their spleen analyzed for size and percentage of neutrophils, macrophages, and NK cells by FACS. Serum from all these mice was collected by exsanguination and hGCSF levels determined by ELISA (Peprotech, UK).

Statistics. GraphPad software (Prism 5.0) and Microsoft Excel was used to plot and analyze all the graphs. Unpaired Student's *t*-test or Mann–Whitney *U*-test was used for most analysis. Statistical analysis of survival curves was performed using Log rank (Mantel-Cox) Test.

SUPPLEMENTARY MATERIAL

Figure S1. % NK and macrophage cells in the spleen.

ACKNOWLEDGMENTS

The authors would like to thank Ron Chakraverty and Derralyn Hughes' groups for providing space and assistance during the Raji disseminated experiment.

A.D. performed the research, with contributions from Y.Z., A.Z.C., and K.B.; A.D. and A.K.F. wrote the paper; A.Z.C., B.P., and Y.Z. provided preliminary data and contributed to writing the manuscript; A.K.F supervised the study. Y.Z., B.P., and A.Z.C. were supported by grant numbers 10011, 07062, and 09026, respectively, from Leukemia Lymphoma Research UK.

The authors declare no competing financial interests.

REFERENCES

1. Grote, D, Russell, SJ, Cornu, TI, Cattaneo, R, Vile, R, Poland, GA *et al.* (2001). Live attenuated measles virus induces regression of human lymphoma xenografts in immunodeficient mice. *Blood* **97**: 3746–3754.
2. Patel, B, Dey, A, Ghorani, E, Kumar, S, Malam, Y, Rai, L *et al.* (2011). Differential cytopathology and kinetics of measles oncolysis in two primary B-cell malignancies provides mechanistic insights. *Mol Ther* **19**: 1034–1040.
3. Russell, SJ, Federspiel, MJ, Peng, KW, Tong, C, Dingli, D, Morice, WG *et al.* (2014). Remission of disseminated cancer after systemic oncolytic virotherapy. *Mayo Clin Proc* **89**: 926–933.

4. Grote, D, Cattaneo, R and Fielding, AK (2003). Neutrophils contribute to the measles virus-induced antitumor effect: enhancement by granulocyte macrophage colony-stimulating factor expression. *Cancer Res* **63**: 6463–6468.
5. Zhang, Y, Patel, B, Dey, A, Ghorani, E, Rai, L, Elham, M *et al.* (2012). Attenuated, oncolytic, but not wild-type measles virus infection has pleiotropic effects on human neutrophil function. *J Immunol* **188**: 1002–1010.
6. Di Carlo, E, Forni, G, Lollini, P, Colombo, MP, Modesti, A and Musiani, P (2001). The intriguing role of polymorphonuclear neutrophils in antitumor reactions. *Blood* **97**: 339–345.
7. Chen, YL, Chen, SH, Wang, JY and Yang, BC (2003). Fas ligand on tumor cells mediates inactivation of neutrophils. *J Immunol* **171**: 1183–1191.
8. Kemp, TJ, Ludwig, AT, Earel, JK, Moore, JM, Vanoosten, RL, Moses, B *et al.* (2005). Neutrophil stimulation with Mycobacterium bovis bacillus Calmette-Guerin (BCG) results in the release of functional soluble TRAIL/Apo-2L. *Blood* **106**: 3474–3482.
9. Breitbach, CJ, Paterson, JM, Lemay, CG, Falls, TJ, McGuire, A, Parato, KA *et al.* (2007). Targeted inflammation during oncolytic virus therapy severely compromises tumor blood flow. *Mol Ther* **15**: 1686–1693.
10. Breitbach, CJ, De Silva, NS, Falls, TJ, Aladl, U, Evgin, L, Paterson, J *et al.* (2011). Targeting tumor vasculature with an oncolytic virus. *Mol Ther* **19**: 886–894.
11. Iankov, ID, Allen, C, Federspiel, MJ, Myers, RM, Peng, KW, Ingle, JN *et al.* (2012). Expression of immunomodulatory neutrophil-activating protein of Helicobacter pylori enhances the antitumor activity of oncolytic measles virus. *Mol Ther* **20**: 1139–1147.
12. Shirafuji, N, Matsuda, S, Ogura, H, Tani, K, Kodo, H, Ozawa, K *et al.* (1990). Granulocyte colony-stimulating factor stimulates human mature neutrophilic granulocytes to produce interferon-alpha. *Blood* **75**: 17–19.
13. Nicola, NA (1987). Why do hemopoietic growth factor receptors interact with each other? *Immunol Today* **8**: 134–140.
14. Mrkic, B, Pavlovic, J, Rülicke, T, Volpe, P, Buchholz, CJ, Hourcade, D *et al.* (1998). Measles virus spread and pathogenesis in genetically modified mice. *J Virol* **72**: 7420–7427.
15. Bendall, LJ and Bradstock, KF (2014). G-CSF: from granulopoietic stimulant to bone marrow stem cell mobilizing agent. *Cytokine Growth Factor Rev* **25**: 355–367.
16. Tamura, M, Hattori, K, Nomura, H, Oheda, M, Kubota, N, Imazeki, I *et al.* (1987). Induction of neutrophilic granulocytosis in mice by administration of purified human native granulocyte colony-stimulating factor (G-CSF). *Biochem Biophys Res Commun* **142**: 454–460.
17. Parameswaran, R, Yu, M, Lim, M, Groffen, J and Heisterkamp, N (2011). Combination of drug therapy in acute lymphoblastic leukemia with a CXCR4 antagonist. *Leukemia* **25**: 1314–1323.
18. Welschinger, R, Liedtke, F, Basnett, J, Dela Pena, A, Juarez, JG, Bradstock, KF *et al.* (2013). Plerixafor (AMD3100) induces prolonged mobilization of acute lymphoblastic leukemia cells and increases the proportion of cycling cells in the blood in mice. *Exp Hematol* **41**: 293–302.e1.
19. Uy, GL, Stock, W, Hsu, YM, Churpek, JE, Westervelt, P, DiPersio J *et al.* (2013). Targeting bone marrow lymphoid niches in acute lymphoblastic leukemia. 1398 (55th ASH annual meeting and exposition, American Society of Hematology, New Orleans).
20. Basnett, J, Cisterne, A, Bradstock, K, Bendall, L. (2012). Effects of G-CSF on acute lymphoblastic leukemia. 2564 (54th ASH annual meeting and exposition, American Society of Hematology, Atlanta, GA).
21. Saito, Y, Uchida, N, Tanaka, S, Suzuki, N, Tomizawa-Murasawa, M, Sone, A *et al.* (2010). Induction of cell cycle entry eliminates human leukemia stem cells in a mouse model of AML. *Nat Biotechnol* **28**: 275–280.
22. Shimazaki, C, Uchiyama, H, Fujita, N, Araki, S, Sudo, Y, Yamagata, N *et al.* (1995). Serum levels of endogenous and exogenous granulocyte colony-stimulating factor after autologous blood stem cell transplantation. *Exp Hematol* **23**: 1497–1502.
23. Castleton, A, Dey, A, Beaton, B, Patel, B, Aucher, A, Davis, DM *et al.* (2014). Human mesenchymal stromal cells deliver systemic oncolytic measles virus to treat acute lymphoblastic leukemia in the presence of humoral immunity. *Blood* **123**: 1327–1335.
24. Kovacs, GR, Parks, CL, Vasilakis, N and Udem, SA (2003). Enhanced genetic rescue of negative-strand RNA viruses: use of an MVA-T7 RNA polymerase vector and DNA replication inhibitors. *J Virol Methods* **111**: 29–36.
25. Bucheit, AD, Kumar, S, Grote, DM, Lin, Y, von Messling, V, Cattaneo, RB *et al.* (2003). An oncolytic measles virus engineered to enter cells through the CD20 antigen. *Mol Ther* **7**: 62–72.
26. Tanaka, H, Okada, Y, Kawagishi, M and Tokiwa, T (1989). Pharmacokinetics and pharmacodynamics of recombinant human granulocyte-colony stimulating factor after intravenous and subcutaneous administration in the rat. *J Pharmacol Exp Ther* **251**: 1199–1203.
27. Frank, T, Klinker, F, Falkenburger, BH, Laage, R, Lühder, F, Göricke, B *et al.* (2012). Pegylated granulocyte colony-stimulating factor conveys long-term neuroprotection and improves functional outcome in a model of Parkinson's disease. *Brain* **135**(Pt 6): 1914–1925.
28. Ohdo, S, Furukubo, T, Arata, N, Yukawa, E, Higuchi, S, Nakano, S *et al.* (1998). Influence of dosing time on pharmacological action of G-CSF in mice. *Life Sciences* **62**, PL163–PL168.
29. Kotto-Kome, AC, Fox, SE, Lu, W, Yang, BB, Christensen, RD and Calhoun, DA (2004). Evidence that the granulocyte colony-stimulating factor (G-CSF) receptor plays a role in the pharmacokinetics of G-CSF and PegG-CSF using a G-CSF-R KO model. *Pharmacol Res* **50**: 55–58.